NeuralEF: Deconstructing Kernels by Deep Neural Networks

Zhijie Deng

Tsinghua University

Contact: dengzhijiethu@gmail.com

Joint work with: Jiaxin Shi and Jun Zhu

Kernel methods

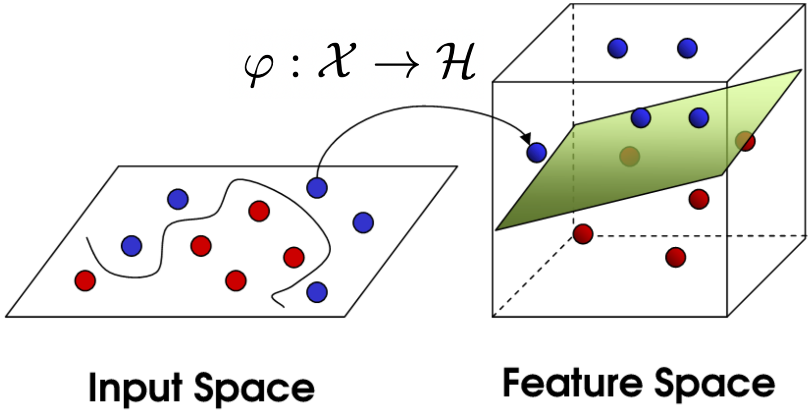

- $\kappa(\boldsymbol{x}, \boldsymbol{x}') = \langle \varphi(\boldsymbol{x}), \varphi(\boldsymbol{x}') \rangle_{\mathcal{H}}$

- Pros: non-parametric flexibility & analytical inference

- Cons: limited scalability – at least O(N^2) complexity, typically O(N^3); inefficiency issue in the test phase

Kernel approximation

- Approximate the kernel with the inner product of some explicit vector representations of the data:

$$\kappa(\boldsymbol{x}, \boldsymbol{x}') \approx \nu(\boldsymbol{x})^\top \nu(\boldsymbol{x}') \qquad \nu : \mathcal{X} \to \mathbb{R}^k$$

- A small k is desired for scalability while the approximation is low-rank

- Popular approaches:
    1. Random Fourier features [Rahimi & Recht, 2007; 2008]
    2. Nystrom method [Nystrom, 1930; Williams & Seeger, 2001]
    3. …

Kernel approximation

Random features (RFs)

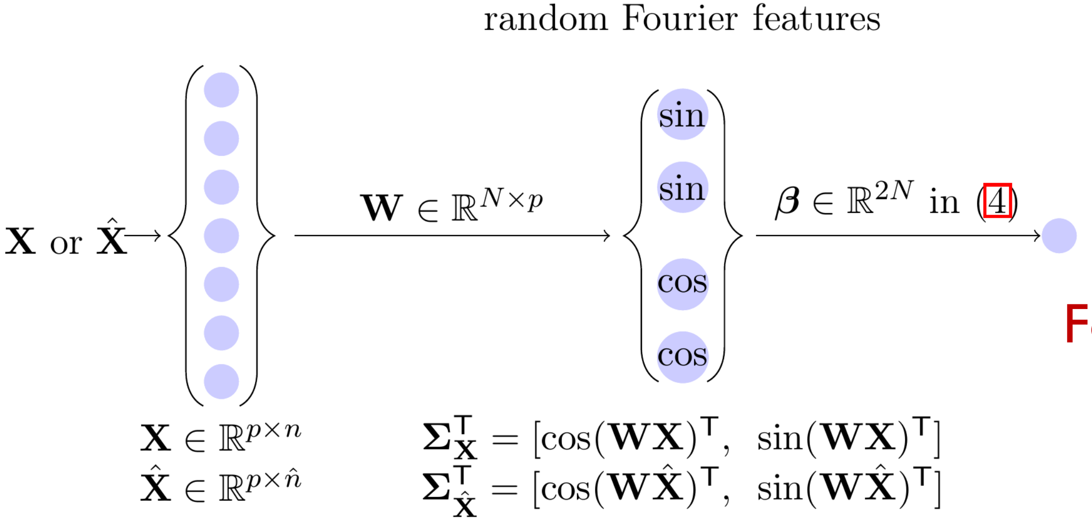

For shift-invariant kernels

[Rahimi et al., 2007]

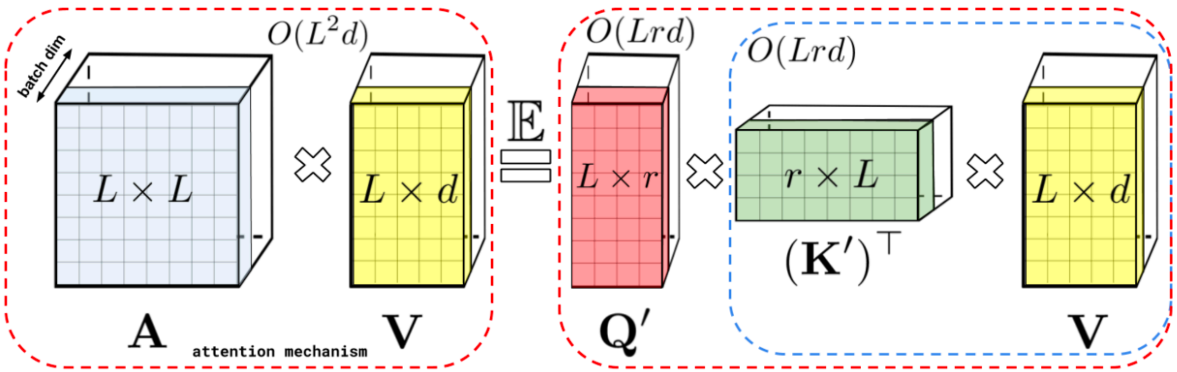

Figure 1: Approximation of the regular attention mechanism **AV** (before $\mathbf{D}^{-1}$-renormalization) via (random) feature maps. Dashed-blocks indicate order of computation with corresponding time complexities attached.

Performer (RFs for exp(x, x’))

[Choromanski et al., 2021]

Kernel approximation

- Mercer's theorem

$$\kappa(\boldsymbol{x}, \boldsymbol{x}') = \sum_{j \geq 1} \mu_j \psi_j(\boldsymbol{x}) \psi_j(\boldsymbol{x}')$$

where ψ_j denote the eigenfunctions of the kernel κ w.r.t. the probability measure q, and $\mu_j \geq 0$ refer to the corresponding eigenvalues

- By the definition of eigenfunction, we have

$$\int \kappa(\boldsymbol{x}, \boldsymbol{x}') \psi_j(\boldsymbol{x}') q(\boldsymbol{x}') d\boldsymbol{x}' = \mu_j \psi_j(\boldsymbol{x}), \ \forall j \geq 1$$

and

$$\int \psi_i(\boldsymbol{x}) \psi_j(\boldsymbol{x}) q(\boldsymbol{x}) d\boldsymbol{x} = \mathbb{1}[i = j], \ \forall i, j \geq 1$$

Kernel approximation
Nystrom method

- Given $\mathbf{X}_{\text{tr}} = \{\boldsymbol{x}_1, ..., \boldsymbol{x}_N\}$ from q, perform MC integration:

$$\frac{1}{N}\sum_{n'=1}^{N}\kappa(\boldsymbol{x}, \boldsymbol{x}_{n'})\psi_j(\boldsymbol{x}_{n'}) = \mu_j\psi_j(\boldsymbol{x}), \forall j \geq 1$$

- Eigendecompose $\kappa(\mathbf{X}_{\text{tr}}, \mathbf{X}_{\text{tr}})$ and get $\{(\hat{\mu}_j, [\hat{\psi}_j(\boldsymbol{x}_1), ..., \hat{\psi}_j(\boldsymbol{x}_N)]^\top)\}_{j=1}^k$

- Kernelized solutions:

$$\hat{\psi}_j(\boldsymbol{x}) = \frac{1}{N\hat{\mu}_j}\sum_{n'=1}^{N}\kappa(\boldsymbol{x}, \boldsymbol{x}_{n'})\hat{\psi}_j(\boldsymbol{x}_{n'}),\ j = 1, ..., k.$$

- Less scalable; the testing entails extensive computes

The modern kernels
Kernels meet NNs

- Classic local kernels suffer from curse of dimensionality [Bengio et al., 2005]

- *Neural network Gaussian process (NNGP) kernels* [Neal, 1995; Lee et al., 2017; Khan et al., 2019]

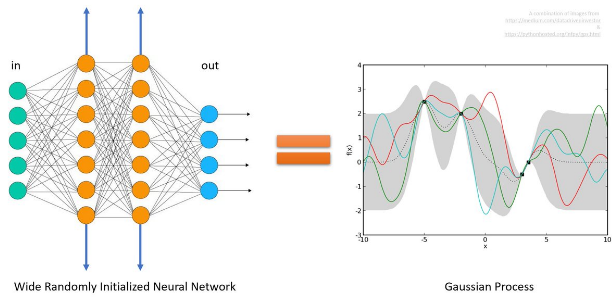

$$\kappa_{\text{NN-GP}}(\boldsymbol{x}, \boldsymbol{x}') = \mathbb{E}_{\boldsymbol{\theta} \sim p(\boldsymbol{\theta})} g(\boldsymbol{x}, \boldsymbol{\theta}) g(\boldsymbol{x}', \boldsymbol{\theta})^\top$$

- *Neural tangent kernels (NTKs)* [Jacot et al., 2018]

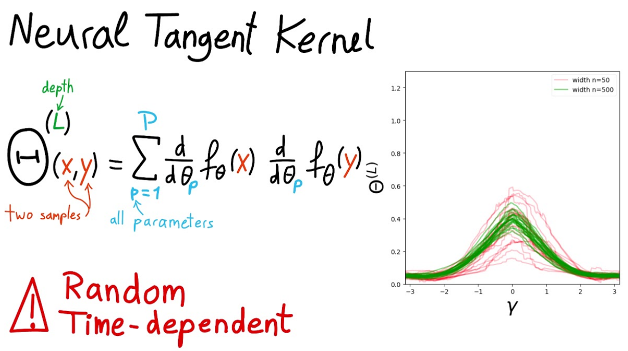

$$\kappa_{\text{NTK}}(\boldsymbol{x}, \boldsymbol{x}') = \partial_{\boldsymbol{\theta}} g(\boldsymbol{x}, \boldsymbol{\theta}) \partial_{\boldsymbol{\theta}} g(\boldsymbol{x}', \boldsymbol{\theta})^\top$$

The modern kernels
Kernels meet NNs

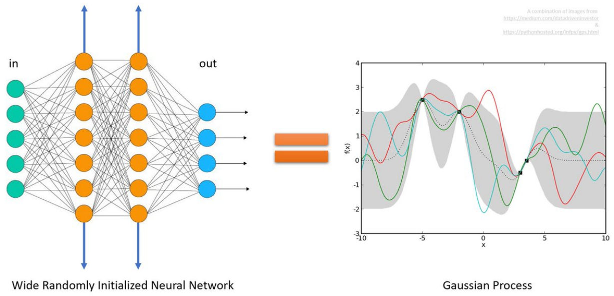

$$\kappa_{\text{NN-GP}}(\boldsymbol{x}, \boldsymbol{x}') = \mathbb{E}_{\boldsymbol{\theta} \sim p(\boldsymbol{\theta})} g(\boldsymbol{x}, \boldsymbol{\theta}) g(\boldsymbol{x}', \boldsymbol{\theta})^\top$$

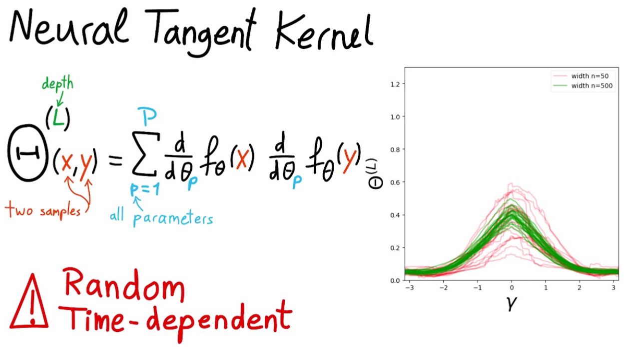

$$\kappa_{\text{NTK}}(\boldsymbol{x}, \boldsymbol{x}') = \partial_{\boldsymbol{\theta}} g(\boldsymbol{x}, \boldsymbol{\theta}) \partial_{\boldsymbol{\theta}} g(\boldsymbol{x}', \boldsymbol{\theta})^\top$$

- Nevertheless, writing down their detailed mathematical formulae is non-trivial [Arora et al., 2019] and evaluating them with recursion is both time and memory consuming.

- They have poor compatibility with standard kernel approximation methods.

NeuralEF: approximate the eigenfunctions of kernels by NNs

Our solution

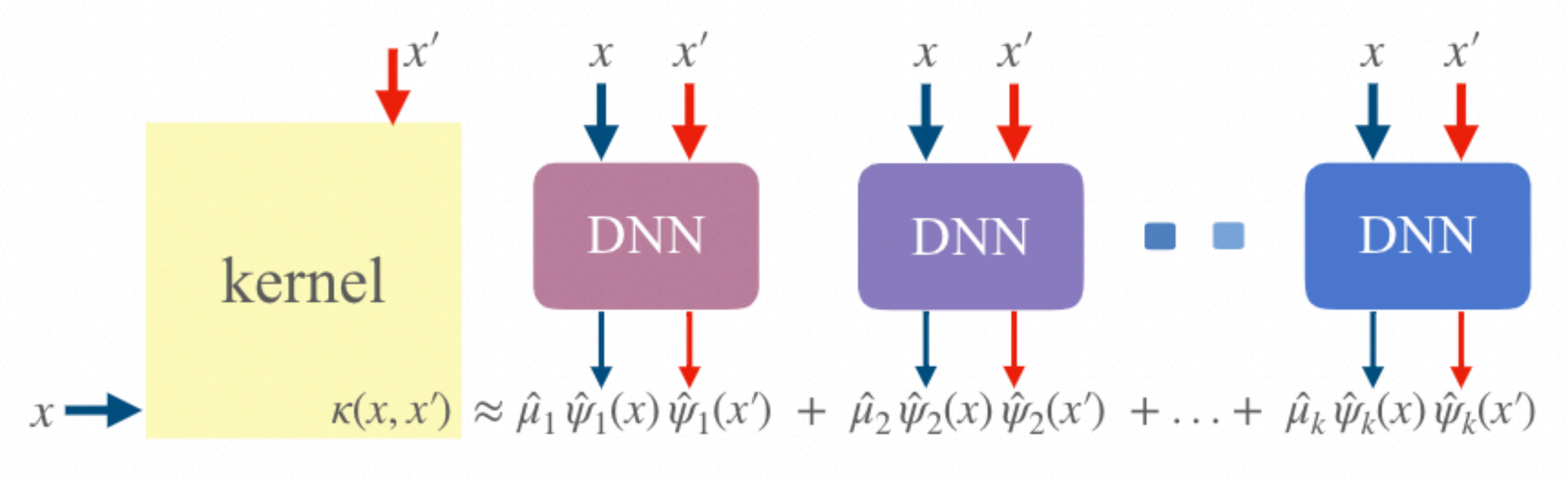

A closely related work

Spectral Inference Networks (SpIN) [Pfau et al., 2018]

- Recover the top eigenfunctions with NNs due to their universal approximation capability and parametric nature
- Introduce a vector-valued NN function $\Psi(\cdot, \boldsymbol{w}) : \mathcal{X} \rightarrow \mathbb{R}^k$ and solve:

$$\max_{\boldsymbol{w}} \operatorname{Tr}\Big(\iint \Psi(\boldsymbol{x}, \boldsymbol{w}) \Psi(\boldsymbol{x}', \boldsymbol{w})^\top \kappa(\boldsymbol{x}, \boldsymbol{x}') q(\boldsymbol{x}) q(\boldsymbol{x}') d\boldsymbol{x} d\boldsymbol{x}' \Big)$$

$$\text{s.t.: } \int \Psi(\boldsymbol{x}, \boldsymbol{w}) \Psi(\boldsymbol{x}, \boldsymbol{w})^\top q(\boldsymbol{x}) d\boldsymbol{x} = \mathbf{I}_k, \qquad (9)$$

- However, this objective makes Ψ recover the subspace spanned by the top-k eigenfunctions rather than the top-k eigenfunctions themselves [Pfau et al., 2018].

A closely related work

Spectral Inference Networks (SpIN) [Pfau et al., 2018]

- Recover the top eigenfunctions with NNs due to their universal approximation capability and parametric nature
- Introduce a vector-valued NN function $\Psi(\cdot, \boldsymbol{w}) : \mathcal{X} \to \mathbb{R}^k$ and solve:

$$\max_{\boldsymbol{w}} \mathrm{Tr}\Big(\iint \Psi(\boldsymbol{x}, \boldsymbol{w})\Psi(\boldsymbol{x}', \boldsymbol{w})^\top \kappa(\boldsymbol{x}, \boldsymbol{x}') q(\boldsymbol{x}) q(\boldsymbol{x}') d\boldsymbol{x} d\boldsymbol{x}' \Big)$$
$$\text{s.t.: } \int \Psi(\boldsymbol{x}, \boldsymbol{w})\Psi(\boldsymbol{x}, \boldsymbol{w})^\top q(\boldsymbol{x}) d\boldsymbol{x} = \mathbf{I}_k, \qquad (9)$$

- To address this issue, SpIN relies on a gradient masking trick which involves a Cholesky decomposition per training iteration.
- SpIN also involves tracking the exponential moving average (EMA) of the Jacobian matrix to debias the stochastic optimization.

Eigendecomposition as asymmetric maximization problems

Our new results

Theorem 1 (Proof in Appendix A.1). *The eigenpairs of the kernel $\kappa(\boldsymbol{x}, \boldsymbol{x}')$ can be recovered by simultaneously solving the following series of constrained maximization problems:*

$$\max_{\hat{\psi}_j} R_{jj} \text{ s.t.: } C_j = 1, R_{1j} = 0, ..., R_{(j-1)j} = 0, \forall j \geq 1, \quad (7)$$

where $\hat{\psi}_j \in L^2(\mathcal{X}, q)$ represent the introduced approximate eigenfunctions, and

$$R_{ij} := \iint \hat{\psi}_i(\boldsymbol{x})\kappa(\boldsymbol{x}, \boldsymbol{x}')\hat{\psi}_j(\boldsymbol{x}')q(\boldsymbol{x}')q(\boldsymbol{x})d\boldsymbol{x}'d\boldsymbol{x}, \quad (8)$$

$$C_j := \int \hat{\psi}_j(\boldsymbol{x})\hat{\psi}_j(\boldsymbol{x})q(\boldsymbol{x})d\boldsymbol{x}. \quad (9)$$

In particular, $(R_{jj}, \hat{\psi}_j)$ will converge to the eigenpair associated with j-th largest eigenvalue of κ.

Generalized Rayleigh quotient

Normalization constraint

Orthogonality constraint

Eigendecomposition as asymmetric maximization problems

Proof scratch--the first problem

- The ground-truth eigenfunctions form a set of orthonormal bases of the L2(X , q) space
- Represent the approximations in such a new axis system $\hat{\psi}_1 = \sum_{i \geq 1} w_i \psi_i$
- The the maximization objective reduces to

$$R_{11} = \sum_{j \geq 1} \mu_j \langle \hat{\psi}_1, \psi_j \rangle^2 = \sum_{j \geq 1} \mu_j \langle \sum_{i \geq 1} w_i \psi_i, \psi_j \rangle^2 = \sum_{j \geq 1} \mu_j w_j^2.$$

- And the constraint reduces to

$$\langle \hat{\psi}_1, \hat{\psi}_1 \rangle = \langle \sum_{i \geq 1} w_i \psi_i, \sum_{j \geq 1} w_j \psi_j \rangle = \sum_{i,j \geq 1} w_i w_j \langle \psi_i, \psi_j \rangle = \sum_{j \geq 1} w_j^2 = 1$$

- It is straight-forward to see the maxima

Eigendecomposition as asymmetric maximization problems

Proof scratch--the second problem

- Given $\hat{\psi}_1 = \psi_1$

$$
\begin{aligned}
& R_{12} = 0 \\
\Rightarrow \quad & \iint \hat{\psi}_1(\boldsymbol{x})\kappa(\boldsymbol{x},\boldsymbol{x}')\hat{\psi}_2(\boldsymbol{x}')q(\boldsymbol{x}')q(\boldsymbol{x})d\boldsymbol{x}'d\boldsymbol{x} = 0 \\
\Rightarrow \quad & \int \hat{\psi}_2(\boldsymbol{x}')q(\boldsymbol{x}') \int \hat{\psi}_1(\boldsymbol{x})\kappa(\boldsymbol{x},\boldsymbol{x}')q(\boldsymbol{x})d\boldsymbol{x}d\boldsymbol{x}' = 0 \\
\Rightarrow \quad & \int \hat{\psi}_2(\boldsymbol{x}')q(\boldsymbol{x}') \int \psi_1(\boldsymbol{x})\kappa(\boldsymbol{x},\boldsymbol{x}')q(\boldsymbol{x})d\boldsymbol{x}d\boldsymbol{x}' = 0 \\
\Rightarrow \quad & \int \hat{\psi}_2(\boldsymbol{x}')q(\boldsymbol{x}')\mu_1\psi_1(\boldsymbol{x}')d\boldsymbol{x}' = 0 \\
\Rightarrow \quad & \langle \psi_1, \hat{\psi}_2 \rangle = 0.
\end{aligned}
$$

- $\hat{\psi}_2$ is constrained in the orthogonal complement of the subspace spanned by ψ_1
- Then we can apply an analysis similar to that for the first problem
- Applying this procedure incrementally to the additional problems then finishes the proof

Eigendecomposition as asymmetric maximization problems

- Slack the constraints on orthogonality as penalties and solve the first k optimization problems

$$\max_{\hat{\psi}_j} R_{jj} - \sum_{i=1}^{j-1} \frac{R_{ij}^2}{R_{ii}} \quad \text{s.t.: } C_j = 1, \text{for } j = 1, ..., k,$$

- Our objective forms a function-space generalization of that in EigenGame [Gemp et al., 2020]

DNNs as eigenfunctions

Use an ensemble of k DNNs to approximate the top-k eigenfunctions

- Mini-batch training -- by MC estimation:

$$\tilde{R}_{ij} = \sum_{b=1}^{B}\sum_{b'=1}^{B}\frac{1}{B^2}\hat{\psi}_i(\boldsymbol{x}_b)\kappa(\boldsymbol{x}_b,\boldsymbol{x}_{b'})\hat{\psi}_j(\boldsymbol{x}_{b'})$$
$$= \frac{1}{B^2}\hat{\boldsymbol{\psi}}_i^{\mathbf{X}\top}\boldsymbol{\kappa}^{\mathbf{X},\mathbf{X}}\hat{\boldsymbol{\psi}}_j^{\mathbf{X}},$$

- L2 Batch normalization (L2BN) to absorb the normalization constraints:

$$h_b^{\text{out}} = \frac{h_b^{\text{in}}}{\sigma}, \text{ with } \sigma = \sqrt{\frac{1}{B}\sum_{b=1}^{B} {h_b^{\text{in}}}^2},\ b = 1, ..., B.$$

- The gradients: $\nabla_{\boldsymbol{w}_j}\ell = -\frac{2}{B^2}\boldsymbol{\kappa}^{\mathbf{X},\mathbf{X}}\left(\hat{\boldsymbol{\psi}}_j^{\mathbf{X}} - \sum_{i=1}^{j-1}\frac{\hat{\boldsymbol{\psi}}_i^{\mathbf{X}\top}\boldsymbol{\kappa}^{\mathbf{X},\mathbf{X}}\hat{\boldsymbol{\psi}}_j^{\mathbf{X}}}{\hat{\boldsymbol{\psi}}_i^{\mathbf{X}\top}\boldsymbol{\kappa}^{\mathbf{X},\mathbf{X}}\hat{\boldsymbol{\psi}}_i^{\mathbf{X}}}\hat{\boldsymbol{\psi}}_i^{\mathbf{X}}\right)\cdot\partial_{\boldsymbol{w}_j}\hat{\boldsymbol{\psi}}_j^{\mathbf{X}}.$

- Extension to *matrix-valued* kernels (e.g., NTKs):
  strategy 1: use multi-output DNNs
  strategy 2: make a factorization assumption

NeuralEF

The algorithm

Algorithm 1 Find the top-k eigenpairs of a kernel by NeuralEF

Input: Training data $\mathbf{X}_{\text{tr}}$, kernel κ, batch size B.
Initialize NNs $\hat{\psi}_j(\cdot) = \hat{\psi}(\cdot, \boldsymbol{w}_j)$ and scalars $\hat{\mu}_j, j \in [k]$;
Compute the kernel matrix $\boldsymbol{\kappa}^{\mathbf{X}_{\text{tr}}, \mathbf{X}_{\text{tr}}} = \kappa(\mathbf{X}_{\text{tr}}, \mathbf{X}_{\text{tr}})$;
for *iteration* **do**
  Draw a mini-batch $\mathbf{X} \subseteq \mathbf{X}_{\text{tr}}$; retrieve $\boldsymbol{\kappa}^{\mathbf{X}, \mathbf{X}}$ from $\boldsymbol{\kappa}^{\mathbf{X}_{\text{tr}}, \mathbf{X}_{\text{tr}}}$;
  Do forward propagation $\hat{\boldsymbol{\psi}}_{\boldsymbol{j}}^{\mathbf{X}} = \hat{\psi}(\mathbf{X}, \boldsymbol{w}_j), j \in [k]$;
  $\hat{\mu}_j \leftarrow \text{EMA}(\hat{\mu}_j, \frac{1}{B^2} \hat{\boldsymbol{\psi}}_{\boldsymbol{j}}^{\mathbf{X}\top} \boldsymbol{\kappa}^{\mathbf{X}, \mathbf{X}} \hat{\boldsymbol{\psi}}_{\boldsymbol{j}}^{\mathbf{X}}), j \in [k]$;
  Compute $\nabla_{\boldsymbol{w}_j} \ell, j \in [k]$ by Equation (18) and do SGD;
end for

Enable the learning of NN-GP kernels and NTKs

Based on thousands of random features

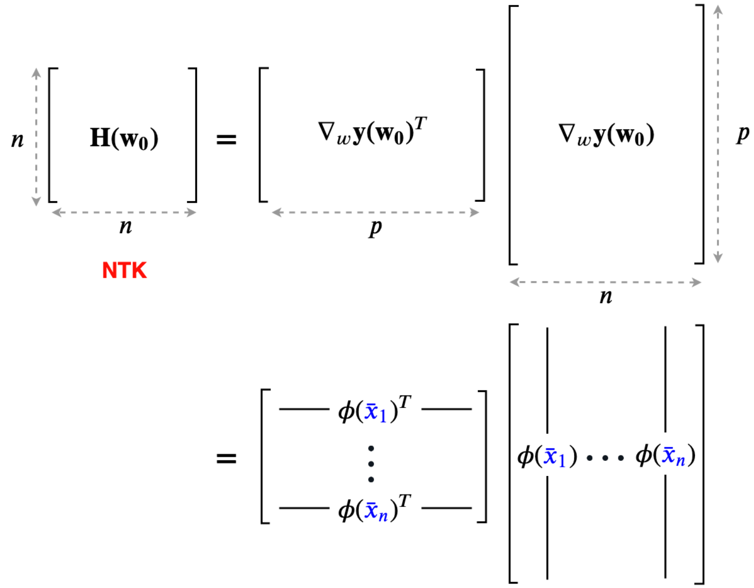

- Computing the training kernel matrices by MC estimation given a distribution $p(v)$ satisfying $\mathbb{E}_{p(\boldsymbol{v})}[\boldsymbol{v}\boldsymbol{v}^\top] = \mathbf{I}_{\dim(\boldsymbol{\theta})}$, then

$$\begin{aligned}\boldsymbol{\kappa}_{\text{NTK}}^{\mathbf{X}_{\text{tr}},\mathbf{X}_{\text{tr}}} &= \mathbb{E}_{\boldsymbol{v}\sim p(\boldsymbol{v})}\left[\partial_{\boldsymbol{\theta}} g(\mathbf{X}_{\text{tr}},\boldsymbol{\theta})\boldsymbol{v}\right]\left[\partial_{\boldsymbol{\theta}} g(\mathbf{X}_{\text{tr}},\boldsymbol{\theta})\boldsymbol{v}\right]^\top \\ &\approx \frac{1}{S}\sum_{s=1}^{S}\left[\frac{g(\mathbf{X}_{\text{tr}},\boldsymbol{\theta}+\epsilon\boldsymbol{v}_s)-g(\mathbf{X}_{\text{tr}},\boldsymbol{\theta})}{\epsilon}\right]\left[\frac{g(\mathbf{X}_{\text{tr}},\boldsymbol{\theta}+\epsilon\boldsymbol{v}_s)-g(\mathbf{X}_{\text{tr}},\boldsymbol{\theta})}{\epsilon}\right]^\top\end{aligned}$$

The impact of NeuralEF

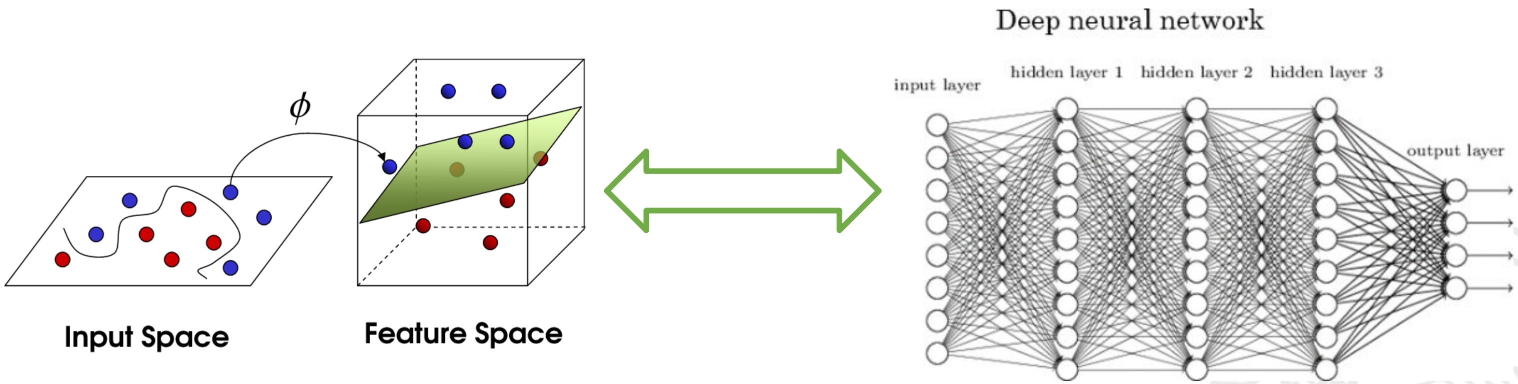

- NeuralEF approximate NTKs and NN-GP kernels with less NN forward passes than RFs
- It gives rise to an unsupervised representation learning paradigm, where the pairwise similarity captured by kernels is embedded into NNs
- It *relates two fields of research*

The applications
Find the eigenfunctions of classic kernels

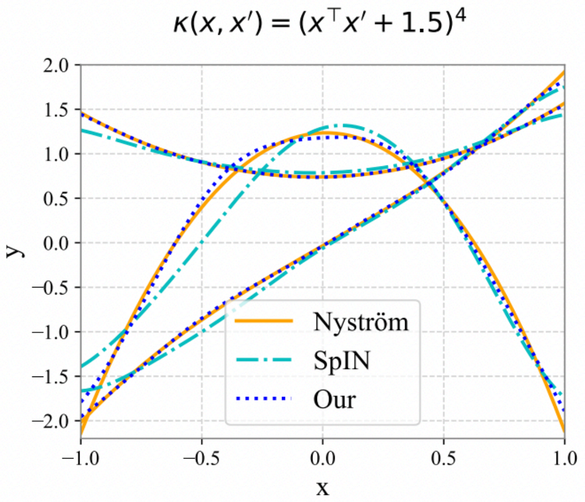

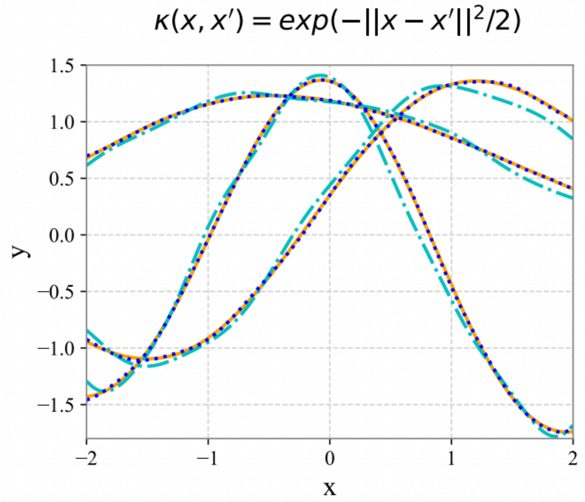

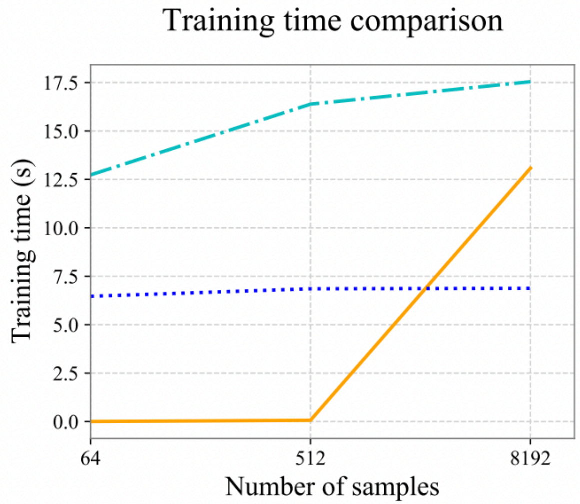

The applications
Process MLP-GP kernels

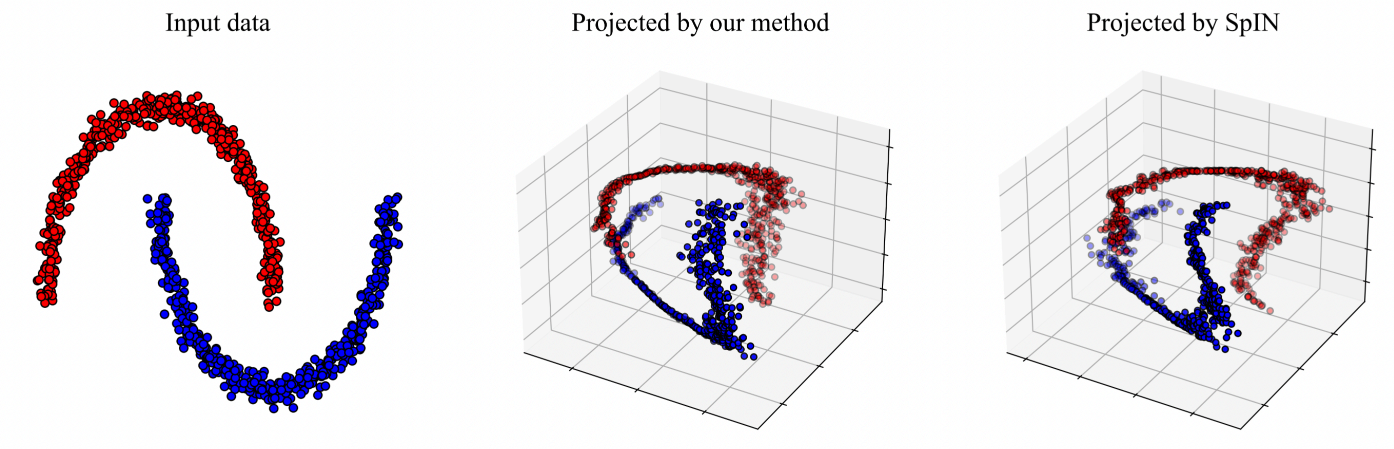

(a) "Two-moon" data

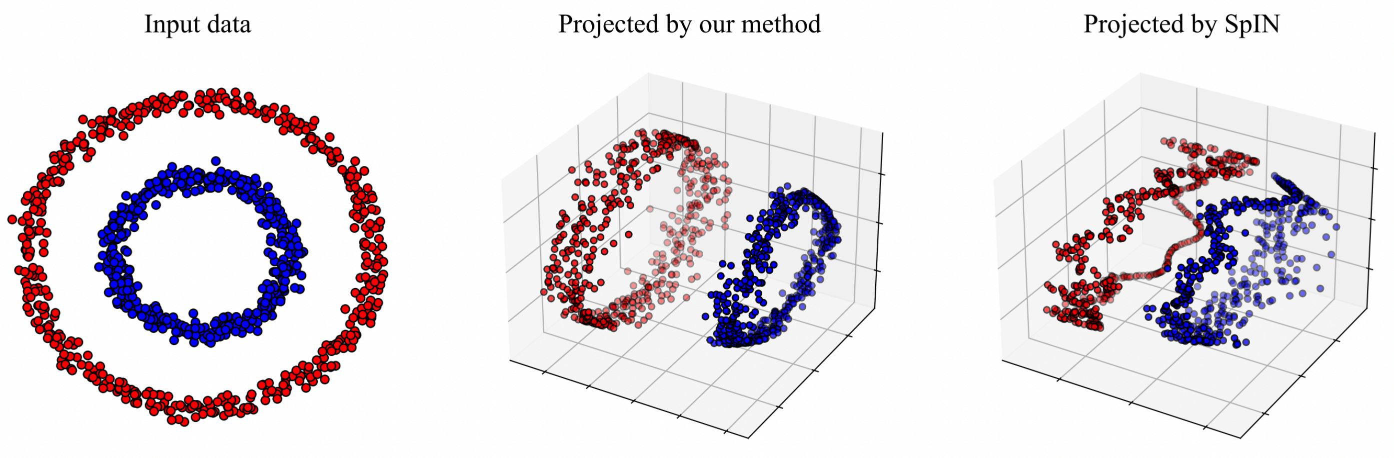

(b) "Circles" data

The applications

Process CNN-GP kernels

Method	LR test accuracy
Our method (CNN-GP kernel)	**84.98%**
Nyström (CNN-GP kernel)	N/A
Nyström (polynomial kernel)	78.00%
Nyström (RBF kernel)	77.55%

The applications
Find the eigenfunctions of NTK which itself is hard to compute

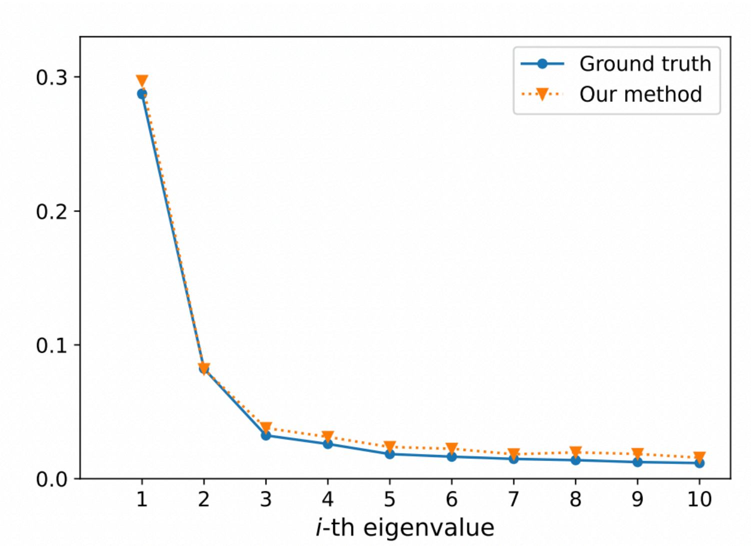

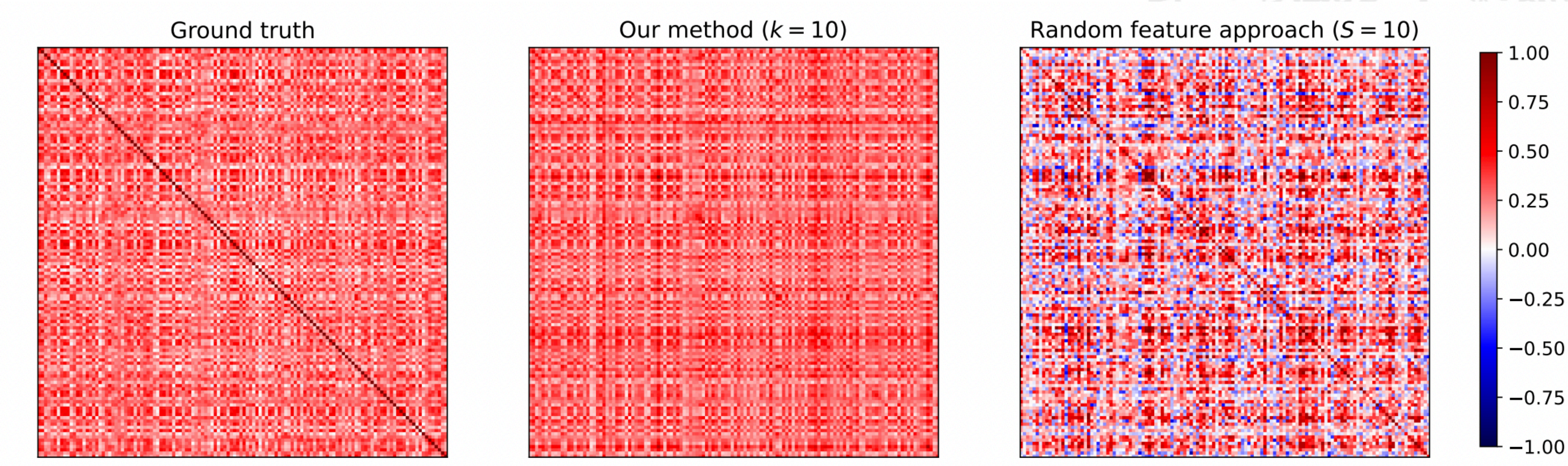

The applications

Improve linearised Laplace approximation with NeuralEF

Inverse of the Gauss-Newton of size # of params × # of params

$$\Sigma^{-1} = \sum_i \partial_\theta g(x_i, \theta_{\text{MAP}})^\top \Lambda_i \partial_\theta g(x_i, \theta_{\text{MAP}}) + 1/\sigma_0^2 I_{\dim(\theta)}$$

$$\mathcal{GP}(f | g(x, \theta_{\text{MAP}}), \partial_\theta g(x, \theta_{\text{MAP}}) \Sigma \partial_\theta g(x', \theta_{\text{MAP}})^\top)$$

By Woodbury matrix identity and Mercer's theorem

$$\mathcal{GP}\left(f | g(x, \theta_{\text{MAP}}), \Psi(x) \left[\sum_i \Psi(x_i)^\top \Lambda_i \Psi(x_i) + \frac{1}{\sigma_0^2} I_k\right]^{-1} \Psi(x')^\top\right),$$

Size: k × k

The concatenation of the k eigenfunctions for the NTK

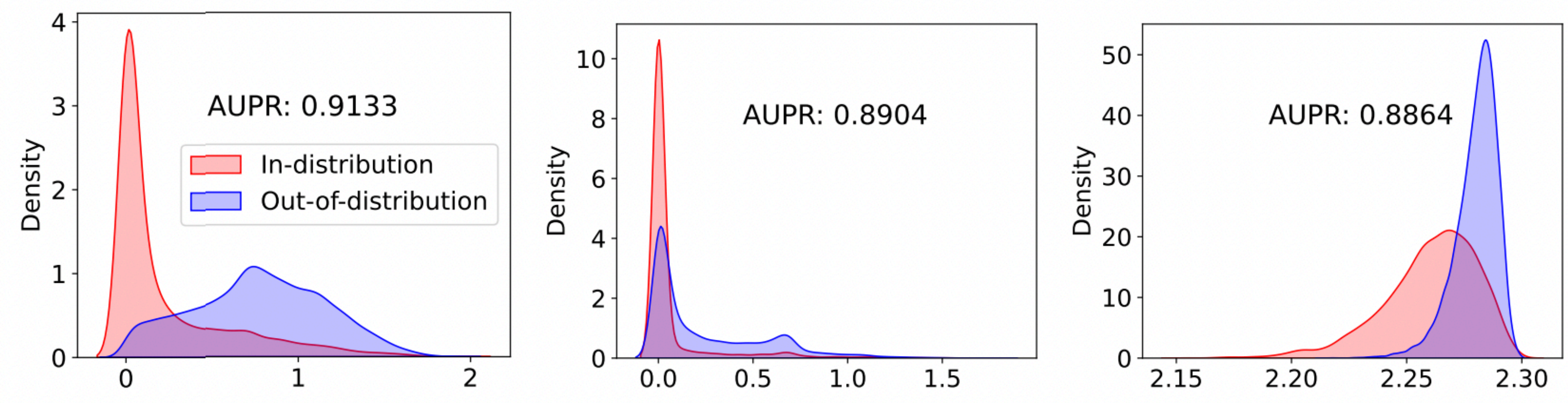

(a) Ours (b) MAP (c) KFAC LLA

The applications

Bayesian deep learning by modeling SGD trajectory

$$\kappa_{\text{SGD}}(\boldsymbol{x}, \boldsymbol{x}') = \frac{1}{M} \sum_{i=1}^{M} \left(g(\boldsymbol{x}, \boldsymbol{\theta}_i) - \bar{g}(\boldsymbol{x})\right) \left(g(\boldsymbol{x}', \boldsymbol{\theta}_i) - \bar{g}(\boldsymbol{x}')\right)^\top$$

$$p(\boldsymbol{x}_{\text{new}}) = \int \mathcal{GP}(f | \bar{g}(\boldsymbol{x}), \kappa_{\text{SGD}}(\boldsymbol{x}, \boldsymbol{x}')) p(\boldsymbol{x}_{\text{new}} | f) df$$

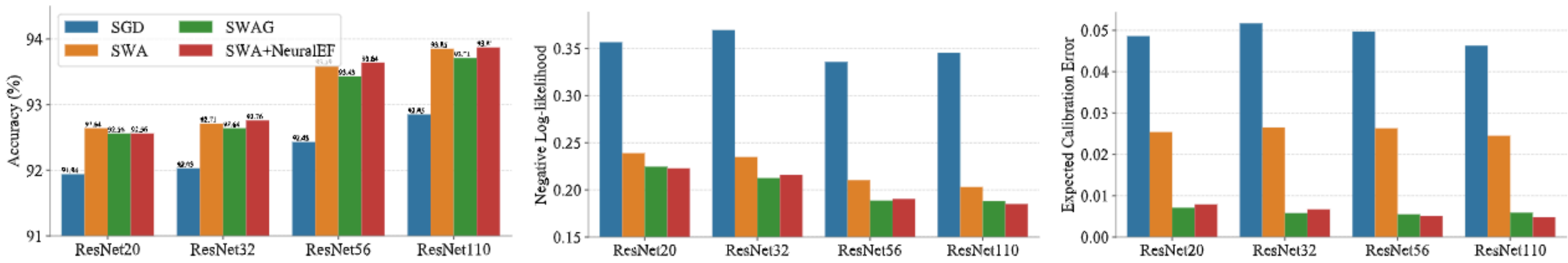

Figure 6: Test accuracy ↑, NLL ↓, and ECE ↓ comparisons among models on CIFAR-10.

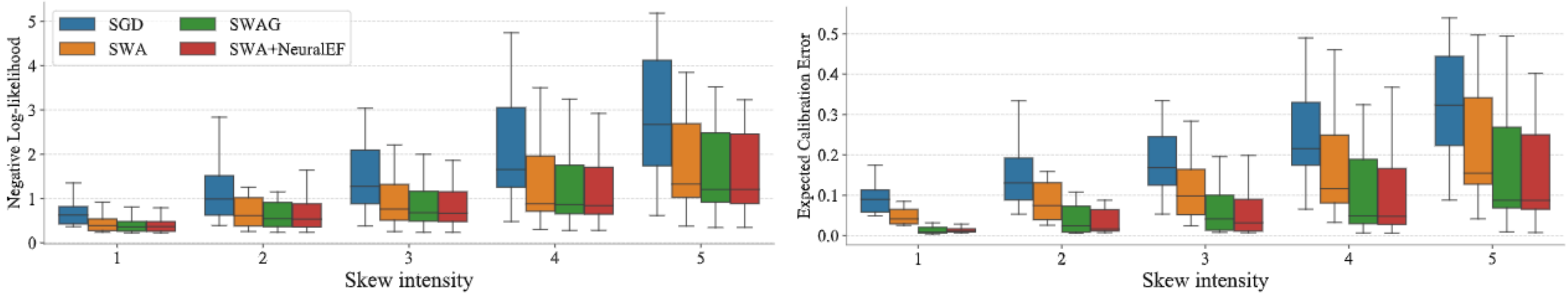

Thanks!